

# The Potential Energy Surface of the H<sub>2</sub>O<sub>2</sub> System

Yingbin Ge<sup>\*1</sup>, Katie Olsen<sup>†</sup>, Ralf I. Kaiser<sup>¶</sup>, and John D. Head<sup>¶1</sup>

<sup>\*</sup>*Ames Laboratory, Iowa State University, Ames, Iowa, 50011*

<sup>†</sup>*School of Chemistry, Georgia Institute of Technology, Atlanta, Georgia, 30332*

<sup>¶</sup>*Department of Chemistry, University of Hawaii at Manoa, Honolulu, Hawaii, 96822*

**Abstract.** The potential energy surfaces (PES) for the singlet and triplet H<sub>2</sub>O<sub>2</sub> molecular system were studied by using the CASSCF, CASPT2, QCISD, QCISD(T), and CCSD(T) methods with the aug-cc-pVDZ, aug-cc-pVTZ, and 6-311+G(3df,2p) basis sets. The CASSCF and CASPT2 results show some significant differences from the QCISD, QCISD(T), and CCSD(T) calculations. The QCISD(T)/QCISD and CCSD(T)/QCISD calculations were found to be suitable for examining most of the species and reaction paths on the H<sub>2</sub>O<sub>2</sub> PES except for a few open shell species which have a multi-reference character. The CASSCF and CASPT2 methods were found to be better suited for treating these open shell species. Consistent with previous theoretical and experimental work we find the hydrogen abstraction reaction <sup>1</sup>O + H<sub>2</sub>O → <sup>2</sup>OH + <sup>2</sup>OH to have a small or no energy barrier suggesting this pathway may have relevance to the astrochemical formation of hydrogen peroxide in an extraterrestrial environment.

**Keywords:** H<sub>2</sub>O<sub>2</sub>, hydrogen peroxide, oxywater, potential energy surface, PES, CASSCF, CASPT2, QCISD, QCISD(T), CCSD(T).

**PACS:** 95.30.Ft Molecular and chemical processes and interactions.

## 1. INTRODUCTION

Singlet and triplet potential energy surfaces of the H<sub>2</sub>O<sub>2</sub> system have been investigated extensively due to their importance for astrochemistry. Recent laboratory experiments investigating the charged particle and ultra violet (UV) photon irradiation of water (H<sub>2</sub>O) ices – the dominant component of ice mantles of dust grains in cold molecular clouds<sup>1</sup> and on the surfaces of small solar system objects such as Kuiper Belt Objects (KBOs)<sup>2,3</sup>, comets, and icy satellites like Europa, Ganymede, and Callisto<sup>4</sup> in the outer solar system showed that a significant fraction of hydrogen peroxide can be generated. Note that water-bonded hydrogen peroxide molecules have been suggested tentatively to be the carrier of the low frequency wing of the 3250 cm<sup>-1</sup> infrared absorption features of the dust grains in cold molecular clouds<sup>5</sup>. Absorption features of hydrogen peroxide have been identified in the infrared and ultraviolet wavelength spectra of Europa, where the hydrogen peroxide concentration is about 0.13 ± 0.07% relative to water<sup>6</sup>. Hendrix et al.<sup>7</sup> reported the existence of hydrogen peroxide on the surfaces of Europa, Ganymede, and Callisto with concentrations of about 0.3% by weight. H<sub>2</sub>O<sub>2</sub> has also been proposed as a precursor molecule to generate molecular oxygen on the surfaces of Ganymede and Europa<sup>8</sup>. However, despite the significance of the hydrogen peroxide molecule in the chemical processing of water-rich ices, little is known on the formation mechanism of the H<sub>2</sub>O<sub>2</sub> molecule. This could be formed either by recombination of two hydroxyl radicals – a radiolysis product of the water molecule – or by addition of an electronically excited oxygen atom to the water molecule yielding an oxywater (H<sub>2</sub>OO) intermediate followed by hydrogen shift and subsequent stabilization of the internally excited hydrogen peroxide molecule in the water matrix<sup>9</sup>. In 1983, Pople et al. first examined the structure of singlet oxywater, <sup>1</sup>H<sub>2</sub>O-O, where the O(<sup>1</sup>D) atom accepts one of the lone pair electrons from O of the water molecule<sup>10</sup>. These calculations suggested that <sup>1</sup>H<sub>2</sub>O-O was an unstable structure since no energy barrier was found for the reaction <sup>1</sup>H<sub>2</sub>O-O → <sup>1</sup>HOOH (hydrogen peroxide) at the MP4/HF level (Single point MP4 energy calculation performed at the HF optimized geometry). However, Bach et al. in 1990 predicted using MP2 optimized geometries a 3.1 kcal/mol energy barrier at the MP4/MP2 level for the same reaction<sup>11</sup>. Likewise, CCSD(T)/CCSD calculations by Schaefer and coworkers agreed with the Bach et al. results by predicting a *ca* 3 kcal/mol energy barrier<sup>12</sup>. More recently, Gonzalez et al. studied the PES of the singlet H<sub>2</sub>O<sub>2</sub> system using the PUMP4/UUMP2 method<sup>13</sup> and the complete active space (CAS) SCF and CASPT2 methods<sup>14</sup>. They found that the energy barrier of the <sup>1</sup>H<sub>2</sub>O-O → <sup>1</sup>HOOH reaction to be 2.8, 7.4, and 0.2 kcal/mol at the PUMP4/UUMP2, CASSCF//CASSCF, and CASPT2//CASSCF levels, respectively. Similarly they found that the predicted values for other energy

<sup>1</sup> Corresponding authors: John D. Head (Email: [johnh@hawaii.edu](mailto:johnh@hawaii.edu)); Yingbin Ge (Email: [yingbin@si.fi.ameslab.gov](mailto:yingbin@si.fi.ameslab.gov)).

barriers and relative energies on the singlet H<sub>2</sub>O<sub>2</sub> PES by these above 3 methods often differ by more than 5 kcal/mol. They argued that the CAS methods should be superior to the MP methods since many of the species of interest have multi-reference characteristics, which cannot be properly described by the single-reference MP methods. However, their CASSCF and CASPT2 results differ significantly from Schaefer et al. CCSD(T) results. It is not surprising that CASSCF cannot predict accurate relative energies since it does not include as much dynamical correlation energy as the CASPT2 and CCSD(T) methods. However the discrepancy between the CASPT2 and CCSD(T) results does raise the question of which method is more suitable for describing the H<sub>2</sub>O<sub>2</sub> potential energy surface. It's also worth noting that Gonzales et al. used a cc-pVTZ basis set in their CASPT2 paper, which inevitably raises another question whether their results are trustworthy since the inclusion of diffuse functions can be critical for predicting reliable energy barriers since many transition states and radical species in the singlet H<sub>2</sub>O<sub>2</sub> system could involve loosely bound electrons. Karkach et al. studied the triplet potential energy surface for H<sub>2</sub>O<sub>2</sub> using the quadratic configuration interaction (QCI) methods (approximation of corresponding coupled cluster methods)<sup>15</sup>. However, it might be expected that the single-reference QCI methods might not correctly describe some open shell species on the H<sub>2</sub>O<sub>2</sub> PES. In this paper, to make comparison between all the aforementioned methods and to study the basis set effects, we have applied the CASSCF<sup>16</sup>, CASPT2<sup>17</sup>, QCISD<sup>18</sup>, QCISD(T)<sup>18</sup>, and CCSD(T)<sup>19</sup> methods to study both of the singlet and triplet H<sub>2</sub>O<sub>2</sub> PES. To evaluate possible basis sets the calculations are performed using 3 different basis sets for calculations, where aug-cc-pVXZ (X=D, T) basis sets<sup>20</sup> include appropriate diffuse functions on the O and H atoms while 6-311+G(3df,2p) includes diffuse functions only on O atoms.

The remainder of the article is organized as follows. In the next section, the various computational methods employed in this paper are briefly described. In the Results and Discussion section, geometric and energetic data are listed and discussed in detail. Singlet and triplet potential energy surfaces of the H<sub>2</sub>O<sub>2</sub> system are also provided to illustrate various reaction paths and energy barriers. The summary and concluding remarks are given in the last section.

## 2. COMPUTATIONAL METHODS

All of the calculations are performed using either the Dunning's aug-cc-pVDZ or aug-cc-pVTZ or 6-311+G(3df,2p) basis sets used in Pople et al. G2 theory<sup>21</sup>. Aug-cc-pVXZ basis sets include diffuse functions on both O and H atoms while the 6-311+G(3df,2p) basis set has diffuse functions only on O atoms. The geometry optimizations for the local minima and transition states are performed at the CASSCF and QCISD levels of theory. Single point energies which include a higher level of electron correlation are obtained at the CASPT2//CASSCF, CCSD(T)//QCISD, and QCISD(T)//QCISD levels of theory using the same basis sets as in the geometry optimization calculations. Full valence active spaces are used in all of the CASSCF and CASPT2 calculations. The active space selected in the CAS calculations for species with an H<sub>m</sub>O<sub>n</sub> stoichiometry consists of m + 6n active electrons and m + 4n active orbitals. Zero point energies (ZPE) are calculated at the QCISD/aug-cc-pVDZ level if not specified. The CASSCF and CASPT2 calculations are carried out using the GAMESS suite of codes<sup>22</sup>. The QCISD, QCISD(T) and CCSD(T) calculations are carried out using the GAUSSIAN 03 package<sup>23</sup>.

## 3. RESULTS AND DISCUSSION

### 3.1. Comparison of Theoretically Predicted Geometries with Experimental Data

Table 1 lists the electronic and structural properties obtained for the various local minima at the CASSCF and QCISD levels of theory using the aug-cc-pVDZ, aug-cc-pVTZ, and 6-311+G(3df,2p) basis sets. The QCISD/aug-cc-pVTZ and QCISD/6-311+G(3df,2p) calculations generally produce the geometries which compare best against the experimental data with the bond length discrepancy being less than 0.01 Å and the angle discrepancy being less than 0.4° with the biggest differences occurring for the hydrogen peroxide ground state. In the HOOH ground state, QCISD finds geometries that are no worse than those from the CASSCF method. The QCISD method with either the aug-cc-pVTZ or 6-311+G(3df,2p) basis set underestimates the O-O bond length by only 0.012 or 0.021 Å. However QCISD with a double zeta aug-cc-pVDZ basis set often slightly overestimates the bond lengths. In contrast, the CASSCF method with all three various basis sets predicts bond lengths which are too large. This overestimation of bond lengths by CASSCF is expected owing to the presence of anti-bonding orbitals in the active space.

### 3.2. Structural types of Local Minima and Transition States

The QCISD optimized structures found for various local isomers and transition states are illustrated in Figure 1. The local minima structures (a) through (h) all have 6 real vibrational frequencies whereas the transition state structures (i)-(o) are characterized by having one imaginary vibrational frequency. Generally, similar structural types are also obtained with the CASSCF method with the main exception occurring for cis-<sup>3</sup>HOOH structure (g). In (g) the predicted O-O bond lengths are 1.895 and 6.397 Å at the QCISD/aug-cc-pVTZ and CASSCF/aug-cc-pVTZ levels of theory, respectively. This big difference demonstrates the failure of the QCISD method at treating open shell species involving large equilibrium bond lengths. The cis-

**TABLE 1.** Comparison between experimental and theoretically predicted geometries for various local minima. Bond lengths are in Å. Bond angles and dihedral angles are in degrees.

Species, Symmetry	CASSCF Geometry <sup>a</sup>	QCISD Geometry <sup>b</sup>	Exp. Geometry <sup>c</sup>
H <sub>2</sub> ( <sup>1</sup> Σ <sub>g</sub> <sup>+</sup> ), D <sub>∞h</sub>	R <sub>HH</sub> : 0.770, 0.755, 0.756	R <sub>HH</sub> : 0.761, 0.743, 0.742	0.741
HO ( <sup>2</sup> Π), C <sub>∞v</sub>	R <sub>HO</sub> : 0.978, 0.975, 0.973	R <sub>HO</sub> : 0.978, 0.971, 0.969	0.970
H <sub>2</sub> O ( <sup>1</sup> A <sub>1</sub> ), C <sub>2v</sub>	R <sub>HO</sub> : 0.967, 0.950, 0.963 ∠HOH: 102.50, 106.26, 103.05	R <sub>HO</sub> : 0.965, 0.959, 0.957 ∠HOH: 104.11, 104.48, 104.71	0.958 104.50
HOO ( <sup>2</sup> A <sub>1</sub> <sup>-</sup> ), C <sub>s</sub>	R <sub>OO</sub> : 1.356, 1.357, 1.347 R <sub>HO</sub> : 0.979, 0.949, 0.974 ∠HOO: 102.88, 103.53, 103.34	R <sub>OO</sub> : 1.348, 1.335, 1.327 R <sub>HO</sub> : 0.977, 0.971, 0.969 ∠HOO: 103.87, 104.28, 104.62	1.331 0.971 104.30
O <sub>2</sub> ( <sup>1</sup> Δ <sub>g</sub> ), D <sub>∞h</sub>	R <sub>OO</sub> : 1.234, 1.231, 1.227	R <sub>OO</sub> : 1.220, 1.211, 1.206	1.216
O <sub>2</sub> ( <sup>3</sup> Σ <sub>g</sub> <sup>+</sup> ), D <sub>∞h</sub>	R <sub>OO</sub> : 1.220, 1.218, 1.215	R <sub>OO</sub> : 1.212, 1.204, 1.200	1.207
HOOH ( <sup>1</sup> A), C <sub>2</sub>	R <sub>OO</sub> : 1.488, 1.479, 1.474 R <sub>HO</sub> : 0.972, 0.969, 0.967 ∠HOO: 98.55, 98.95, 99.13 ∠HOOH: 114.25, 115.29, 112.28	R <sub>OO</sub> : 1.462, 1.444, 1.435 R <sub>HO</sub> : 0.969, 0.964, 0.962 ∠HOO: 100.02, 100.52, 100.82 ∠HOOH: 111.72, 111.62, 111.01	1.456 0.967 102.32 113.70

- a. Geometric parameters calculated at the CASSCF level of theory with the aug-cc-pVDZ, aug-cc-pVTZ, and 6-311+G(3df,2p) basis sets, respectively.  
 b. Geometric parameters calculated at the QCISD level of theory with the aug-cc-pVDZ, aug-cc-pVTZ, and 6-311+G(3df,2p) basis sets, respectively.  
 c. Experimental data are obtained from reference 24.

<sup>3</sup>HOOH is formed from triplet bonded OH radicals, where the two single unpaired electrons on the O atoms each have the same spin state which, because of the Pauli exclusion principle, are unable to pair up to form a single bond. The major interactions between the 2 OH groups are derived from the expected attractive dispersion force balanced against the dipole-dipole repulsion, suggesting that the long O-O distance predicted by CASSCF is the more reasonable result.

Transition state <sup>1</sup>TS1 (i) connects to the local minima <sup>1</sup>H<sub>2</sub>O-O (a) and <sup>1</sup>HOOH (e). <sup>3</sup>TS1 (j) connects with <sup>3</sup>O-H<sub>2</sub>O (d) and <sup>3</sup>HOOH (f) structures. <sup>1</sup>TS2 (k) connects with oxywater <sup>1</sup>H<sub>2</sub>O-O (a) and separated H<sub>2</sub> and <sup>1</sup>O<sub>2</sub> molecules. <sup>3</sup>TS2 (l) connects with <sup>3</sup>H<sub>2</sub>O-O (b) and a separated <sup>2</sup>H atom and a <sup>2</sup>HOO radical. <sup>1</sup>TS3 (m) connects with ground state <sup>1</sup>HOOH (e) and separated H<sub>2</sub> and <sup>1</sup>O<sub>2</sub> molecules. We note that the transition state <sup>1</sup>TS3 structure (m) was only found at the HF and B3LYP levels but not at the CASSCF or QCISD level. The <sup>3</sup>TS4 (n) and <sup>3</sup>TS5 (o) transition states connects with the trans- (f) or cis- (g) <sup>3</sup>HOOH, respectively, and the separated <sup>2</sup>H atom and <sup>2</sup>HOO radical.

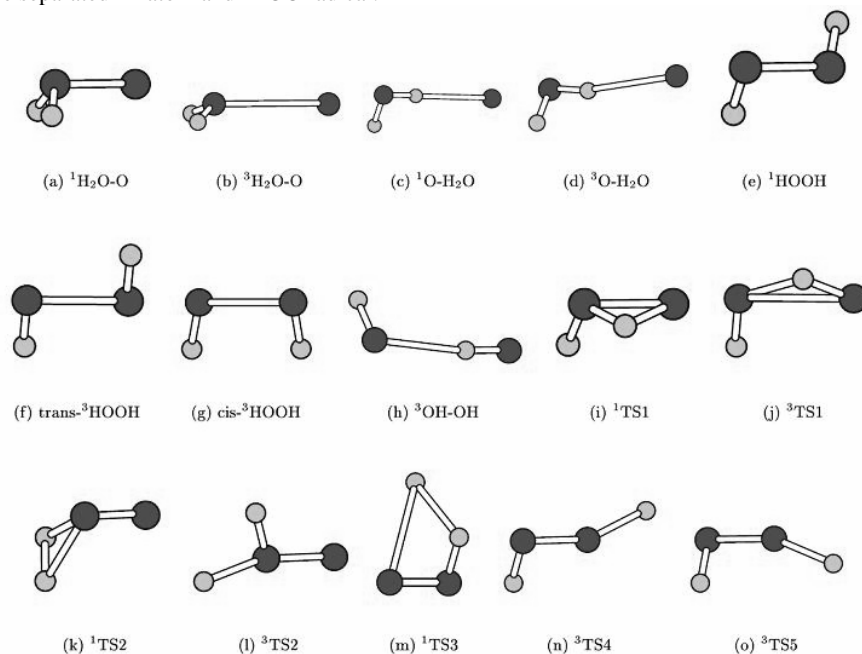


**FIGURE 1.** QCISD optimized H<sub>2</sub>O<sub>2</sub> local isomer and transition state structures. The Cartesian coordinates for all of the structures are available upon request.

### 3.3. O and O<sub>2</sub> triplet-singlet splitting

Figure 2 compares O (<sup>3</sup>P to <sup>1</sup>D) and O<sub>2</sub> (<sup>3</sup>Σ<sub>g</sub><sup>+</sup> to <sup>1</sup>Δ<sub>g</sub>) triplet-singlet excitation energies obtained by the different computation methods against the corresponding experimental data. Figure 2 shows the CASPT2 method with the aug-cc-pVTZ and 6-311+G(3df,2p) basis sets gives, to within 2 kcal/mol, the closest agreement with the experimental data. The CASSCF calculations also predict reasonable triplet-singlet splitting. However, both the QCISD(T)/QCISD and CCSD(T)/QCISD methods overestimate the O and O<sub>2</sub> triplet-singlet splitting by around 3 and 7 kcal/mol, respectively. The most likely cause for the discrepancies between the QCI or CC results and the experimental values is that the energies of the open-shell singlet O and O<sub>2</sub> are too high because of their multi-reference characteristics which cannot be accurately described by the single-reference QCI and CC methods.

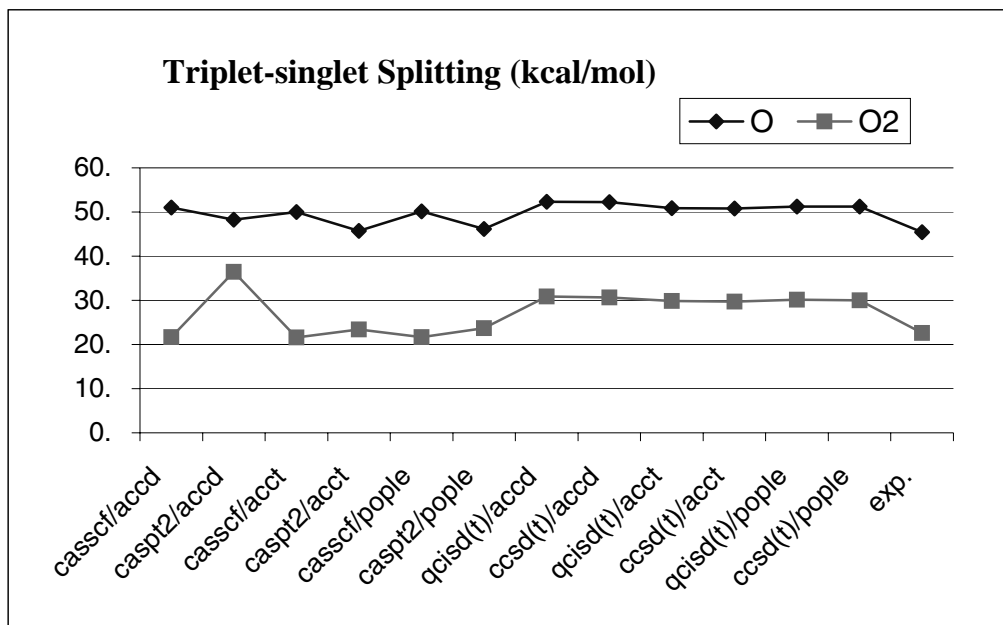


**FIGURE 2.** O and O<sub>2</sub> triplet-singlet splitting energies (in kcal/mol) using various computation methods compared with experimental values<sup>25</sup>. The aug-cc-pVDZ, aug-cc-pVTZ, and 6-311+G(3df, 2p) basis sets are abbreviated by accd, acct, and pople, respectively.

### 3.4. Singlet and Triplet H<sub>2</sub>O-O

The calculations by Schaefer et al., Bach et al., and Gonzales et al. suggest that singlet oxywater can be converted to hydrogen peroxide by overcoming a *ca* 0.2-7.4 kcal/mol energy barrier via the <sup>1</sup>TS1 transition state. Our QCISD(T) and CCSD(T) calculations with a aug-cc-pVTZ basis set suggest *ca* 3.5, and 3.9 kcal/mol energy barrier respectively with ZPE correction, being consistent with the Bach et al. and Schaefer et al. results. However, our CASSCF and CASPT2 methods predict only 1.9 and 0.6 kcal/mol energy barriers without ZPE correction, and these energy barriers become -1.1 and -2.3 kcal/mol after inclusion of the ZPE. This discrepancy is not very surprising since CASSCF and even CASPT2 methods do not recover as much correlation energy as QCISD(T) or CCSD(T) does. It has been pointed out that the CASPT2 method recovers both non-dynamical and dynamical correlation energies but still produces 3-6 kcal/mol relative energy error per broken electron pair<sup>26</sup>. Thus in the rest of this paper, we will use the more accurate CCSD(T)/aug-cc-pVTZ results unless the species to be described involve considerable multi-reference character which needs to be described more properly by the CAS methods. CCSD(T) calculations also show that the <sup>1</sup>H<sub>2</sub>O-O molecule is about 34-35 kcal/mol more stable than the separate water molecule and O(<sup>1</sup>D) atom but 16-17 kcal/mol less stable than H<sub>2</sub>O and a separate O(<sup>3</sup>P) atom. In the geometry optimization of <sup>3</sup>H<sub>2</sub>O-O we found the O-O bond is much longer than in <sup>1</sup>H<sub>2</sub>O-O raising the question whether the <sup>3</sup>H<sub>2</sub>O-O structure has as deep a well as in the <sup>1</sup>H<sub>2</sub>O-O local minimum. With the ZPE correction, we find <sup>3</sup>H<sub>2</sub>O-O lies only 0.8 kcal/mol lower in energy than separate water and O(<sup>3</sup>P) atom at the CCSD(T) level with all three aug-cc-pVDZ, aug-cc-pVTZ, and Pople's 6-311+G(3df, 2p) basis sets. This binding energy is further reduced to *ca* 0.5 kcal/mol when the basis set superposition error (BSSE) is considered. We found no energy barrier between <sup>3</sup>H<sub>2</sub>O-O and the separate H<sub>2</sub>O + <sup>3</sup>O. It is reasonable to conclude that <sup>3</sup>H<sub>2</sub>O-O is a molecular complex where the two O atoms have less than 1 kcal/mol van der Waals interaction. The different O-O bonding characteristics in the <sup>1</sup>H<sub>2</sub>O-O and <sup>3</sup>H<sub>2</sub>O-O species can be understood by examining the valence orbitals of the O(<sup>1</sup>D) and O(<sup>3</sup>P) atoms. The O(<sup>1</sup>D) can have all six valence electrons paired, so that only 3 of the 4 available valence orbitals are occupied. The last empty valence orbital of the O(<sup>1</sup>D) atom can accept a lone electron pair donated from the water O atom to form an ylide bond. The O(<sup>3</sup>P) atom has the 4 valence orbitals either doubly or singly occupied and thus is unable to accept a complete lone pair from the water O atom electrons as the O(<sup>1</sup>D)

does. The above explanation is partly confirmed by a Mulliken population analysis at the QCISD(T) and CCSD(T) level with a aug-cc-pVTZ basis set. The O atom bonded to water bears a -0.42 Mulliken charge in  $^1\text{H}_2\text{O}-\text{O}$  but a 0.0 charge in  $^3\text{H}_2\text{O}-\text{O}$ .

### 3.5. H-Abstraction Reaction: $\text{O}(^1\text{D}) + \text{H}_2\text{O} \rightarrow ^2\text{OH} + ^2\text{OH}$

Theoretical calculations at the CASSCF/cc-pVTZ level of theory done by Gonzales et al.<sup>14</sup> and experimental evidence<sup>27</sup> has lead to the conclusion that the H abstraction reaction  $^1\text{O} + \text{H}_2\text{O} \rightarrow ^2\text{OH} + ^2\text{OH}$  has no energy barrier. We have found a 2<sup>nd</sup>-order transition state for the H abstraction reaction at the CASSCF(14,10)/aug-cc-pVTZ level. It has a 4410i  $\text{cm}^{-1}$  imaginary vibrational mode which moves the central H atom in the TS between two different but equivalent oxywater structures. The second imaginary frequency at 2802i  $\text{cm}^{-1}$  corresponds to the H abstraction reaction shown in Figure 3. Due to lack of the size-consistency of the CASSCF methods, we compared the relative energy of the 2<sup>nd</sup>-order TS with  $^1\text{O}-\text{H}_2\text{O}$  instead of separate  $\text{O}(^1\text{D})$  and  $\text{H}_2\text{O}$ . The 2<sup>nd</sup>-order transition state lies 1.8 kcal/mol higher than  $^1\text{O}-\text{H}_2\text{O}$  at the CASSCF/aug-cc-pVTZ level without ZPE being included. The inclusion of dynamic correlation energy by performing the CASPT2//CASSCF/aug-cc-pVTZ calculation shows that the 2<sup>nd</sup>-order TS is 1.6 kcal/mol more stable than the  $^1\text{O}-\text{H}_2\text{O}$  local minimum. The reason why the TS has lower energy than the product could be due to the dual level CASPT2//CASSCF method we use, which computes CASPT2 single point energy using a lower level CASSCF geometry. Nonetheless it still serves as an indirect evidence supporting that the  $^1\text{O} + \text{H}_2\text{O} \rightarrow ^2\text{OH} + ^2\text{OH}$  reaction has very small or no energy barrier if a 1<sup>st</sup>-order TS does exist for the reaction, agreeing well with Gonzales et al. theoretical calculations<sup>14</sup> and the experimental results<sup>27</sup>. The two product  $^2\text{OH}$  radicals in the gas phase reaction will simply separate from each other but in a condensed phase the two  $^2\text{OH}$  radicals could subsequently recombine to form hydrogen peroxide and this pathway might provide an alternative to the radiolysis of water for the source of  $^2\text{OH}$  radicals.

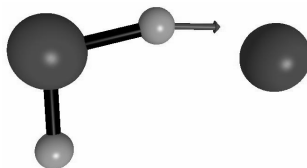


FIGURE 3. The 2802i  $\text{cm}^{-1}$  imaginary frequency mode in the 2<sup>nd</sup>-order TS that connects the  $^1\text{O} + \text{H}_2\text{O} \rightarrow ^2\text{OH} + ^2\text{OH}$  reaction.

### 3.6. Insertion Reaction: $\text{O}(^1\text{D}) + \text{H}_2\text{O} \rightarrow ^1\text{HOOH}$

It was proposed that  $\text{O}(^1\text{D})$  can insert into a Si-H bond of  $\text{SiH}_4$ <sup>28</sup> or C-C or C-H bond of cyclopropane<sup>29</sup> without overcoming any energy barrier. We have examined the  $^1\text{O} + \text{H}_2\text{O} \rightarrow ^1\text{HOOH}$  reaction path using the fast B3LYP methods as a starting point. No direct insertion reaction path was found at the B3LYP level. Since this reaction path has a multi-reference nature we further examined the reaction path at CASSCF/aug-cc-pVTZ level. We find that if the  $\text{O}(^1\text{D})$  atom attacks the water molecule on roughly the opposite side from the 2 H atoms, singlet oxywater is formed without any energy barrier. While if  $\text{O}(^1\text{D})$  attacks the H side of the water molecule, the H abstraction reaction discussed in (3.5) takes place to produce 2  $^2\text{OH}$  radicals overcoming very small or no energy barrier.

### 3.7. Singlet and Triplet Potential Energy Surfaces

Triplet and singlet potential energy surfaces for the  $\text{H}_2\text{O}_2$  system computed by the CCSD(T)//QCISD/aug-cc-pVTZ method are summarized in figure 4. The Gibbs free energies (kcal/mol) at 0 K (since  $T = 0$  K, Gibbs energies coincide with enthalpies) are all taken relative to the  $\text{O}(^3\text{P}) + \text{H}_2\text{O}$  ground state energy. All of the ZPE values were obtained at the QCISD/aug-cc-pVDZ levels except that the ZPE of  $^1\text{TS2}$  was obtained at the QCISD/6-311+G(3df,2p) level. It is worth noting that on the triplet PES the cis- $^3\text{HOOH}$  and trans- $^3\text{HOOH}$  structures have 4.7 and 0.1 kcal/mol higher energies than 2 separate  $^2\text{OH}$  radicals. These higher energies are partly due to the inability of the CCSD(T) method to treat accurately species with multireference character and partly due to the higher ZPE values of the cis- $^3\text{HOOH}$  and trans- $^3\text{HOOH}$  relative to that for 2  $^2\text{OH}$  radicals. Limitations on the accuracy of the calculations make it impractical to locate TS structures interconnecting the cis- $^3\text{HOOH}$ , trans- $^3\text{HOOH}$ ,  $^3\text{OH}-\text{OH}$  and the 2 separate  $^2\text{OH}$  radicals. The other predicted relative energies in the triplet PES are all found to be within 2 kcal/mol of the values obtained by Karkach et al<sup>15</sup>. We will not further discuss the triplet PES since Karkach et al. gave very detailed discussions in their paper<sup>15</sup>. The oxywater  $^1\text{H}_2\text{O}-\text{O}$  and  $^1\text{O}-\text{H}_2\text{O}$  local minima are formed with no energy barrier from  $\text{O}(^1\text{D})$  and water. The  $^1\text{TS1}$  transition state shows that the singlet oxywater must overcome a 3-4 kcal/mol energy barrier to form hydrogen peroxide.  $^1\text{TS2}$  connects the singlet oxywater to the separate  $\text{H}_2$  and  $^1\text{O}_2$  molecules. However, the high energy barriers in both the forward and backward directions suggests that a reaction through  $^1\text{TS2}$  will not be as competitive as some of the other reactions which take place on the singlet surface. We have located the  $^1\text{TS3}$  connecting  $^1\text{HOOH}$  to the separate  $\text{H}_2$  and  $^1\text{O}_2$  molecules only at the B3LYP and HF level and consequently we do not provide a relative energy for  $^1\text{TS3}$  in the PES. The forward and reverse energy barriers of  $^1\text{HOOH} \rightarrow \text{H}_2$  and  $^1\text{O}_2$  are 85.3 and 17.2 kcal/mol at the CCSD(T)//B3LYP/aug-cc-pVTZ level. The  $^1\text{TS4}$  is a 2<sup>nd</sup>

order transition state with 2 imaginary frequencies, where the  $2802i\text{ cm}^{-1}$  imaginary frequency corresponds to the  $^1\text{O} + \text{H}_2\text{O} \rightarrow ^2\text{OH} + ^2\text{OH}$  reaction path with a small or no energy barrier.

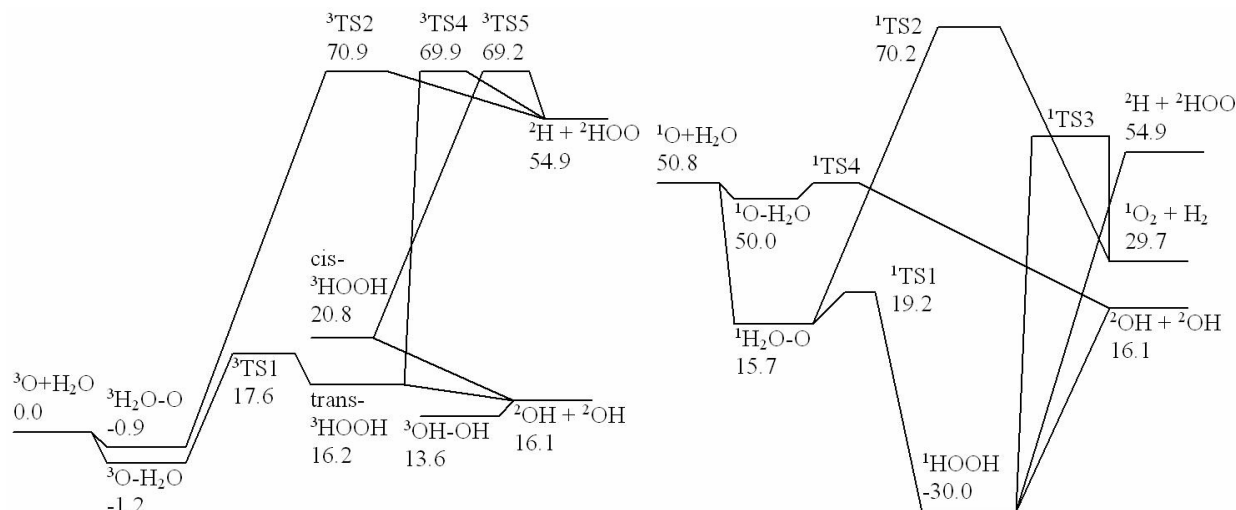


**FIGURE 4.** Potential energy surfaces of the triplet (left) and singlet (right)  $\text{H}_2\text{O}_2$  systems calculated with the CCSD(T)//QCISD/aug-cc-pVTZ method. The energies (in kcal/mol) of the singlet and triplet species are all relative to the  $\text{O}(^3\text{P}) + \text{H}_2\text{O}$  ground state energy.

## 4. CONCLUSION

The multireference CASSCF and CASPT2 methods were compared carefully against the single-reference QCISD, QCISD(T), and CCSD(T) methods for both the singlet and triplet  $\text{H}_2\text{O}_2$  systems. We found that the QCISD method predicts geometries very close to the experimental values and accurate single point energies for many of the species on the  $\text{H}_2\text{O}_2$  PES of system can routinely be obtained from the QCISD(T)//QCISD or CCSD(T)//QCISD calculations provided a fairly large basis set, such as aug-cc-pVTZ, is used. However the CASPT2//CASSCF method should be applied for transitions and/or reactions, such as the O and  $\text{O}_2$  triplet-singlet splitting, that involve species which have significant multi-reference characteristics. The direct insertion reaction  $^1\text{O} + \text{H}_2\text{O} \rightarrow ^1\text{HOOH}$  was studied using the B3LYP and CASSCF methods. Unlike methane, the O atom in the water bears two lone pairs of electrons one of which can readily form a ylide bond with the  $\text{O}(^1\text{D})$  atom, thereby preventing the direct insertion reaction from taking place. The H abstraction reaction  $^1\text{O} + \text{H}_2\text{O} \rightarrow ^2\text{OH} + ^2\text{OH}$  was also studied at the CASSCF(14,10)/aug-cc-pVTZ and CASPT2//CASSCF/aug-cc-pVTZ levels. Small or no energy barrier was found for the reaction in agreement with previous theoretical and experimental results; and in the condensed phase the H abstraction reaction may be a low energy pathway providing a source of pairs of OH radicals which can recombine to form  $^1\text{HOOH}$ .

## 5. ACKNOWLEDGMENTS

The authors would like to thank the Maui High Performance Computing Center for providing ample CPU time. Olsen was supported by the NSF-REU program award number CHE03-53251.

## 6. REFERENCES

1. P. Ehrenfreund, C. Krafft, H. Kochan, and V. Pirronello, *Laboratory astrophysics and space research* (Boston: Kluwer Academic Publishers 1999).
2. C. de Bergh, *Astrophysics and Space Science Library* **305**, 205 (2004).
3. D. C. Jewitt and J. Luu, *Nature* **432**, 731 (2004).
4. S. R. Taylor, *Solar system evolution: a new perspective: an inquiry into the chemical composition, origin, and evolution of the solar system* (2nd ed.; Cambridge; New York: Cambridge University Press 2001).
5. A. G. G. M. Tielens, and W. Hagen, *Astronomy and Astrophysics* **114**, 245 (1982).
6. R. W. Carlson, M. S. Anderson, R. E. Johnson, W. D. Smythe, A. R. Hendrix, C. A. Barth, L. A. Soderblom, G. B. Hansen, T. B. McCord, J. B. Dalton, R. N. Clark, J. H. Shirley, A. C. Ocampo, and D. L. Matson, *Science* **283**, 2062 (1999).

7. A. R. Hendrix, C. A. Barth, A. I. F. Stewart, C. W. Hord, and A. L. Lane, in *Lunar and Planetary Institute Conference Abstracts, Hydrogen Peroxide on the Icy Galilean Satellites*, 2043 (1999).
8. M. T. Sieger, W. C. Simpson, and T. M. Orlando, *Nature* **394**, 554 (1998).
9. W. Zheng, D. C. Jewitt, and R. I. Kaiser, *Astrophysical Journal* **639**, 534 (2006).
10. J. A. Pople, K. Raghavachari, M. J. Frisch, J. S. Binkley, and P. v. R. Schleyer, *J. Am. Chem. Soc.* **105**, 6089 (1983).
11. R. D. Bach, J. J. W. McDouall, A. L. Owensby, and H. B. Schlegel, *J. Am. Chem. Soc.* **112**, 7065 (1990).
12. C. Meredith, T. P. Hamilton, and H. F. Schaefer III, *J. Phys. Chem.* **92**, 9250 (1992).
13. R. Sayos, C. Oliva, and M. Gonzales, *J. Chem. Phys.* **113**, 6736 (2000).
14. R. Sayos, C. Oliva, and M. Gonzales, *J. Chem. Phys.* **115**, 8828 (2001).
15. S. P. Karkach and V. I. Osherov, *J. Chem. Phys.* **110**, 11918 (1999).
16. B. O. Roos, in *Methods in Computational Molecular Physics*, edited by G. H. F. Diercksen and S. Wilson (Reidel, Dordrecht, Netherlands, 1983), pp 161.
17. K. Andersson, P.-A. Malmqvist, B. O. Roos, A. J. Sadlej, and K. Wolinski, *J. Phys. Chem.* **94**, 5483 (1990)
18. J. A. Pople, M. Head-Gordon, and K. Raghavachari, *J. Chem. Phys.* **87**, 5968 (1987).
19. K. Raghavachari, G. W. Trucks, J. A. Pople, and M. Head-Gordon, *Chem. Phys. Lett.* **157**, 479 (1989).
20. T. H. Dunning, Jr. *J. Chem. Phys.* **90**, 1007 (1989).
21. L. A. Curtiss, K. Raghavachari, G. W. Trucks, and J. A. Pople, *J. Chem. Phys.* **94**, 7221 (1991).
22. GAMESS, The General Atomic and Molecular Electronic Structure System, M. W. Schmidt, K. K. Baldrige, J. A. Boatz, S. T. Elbert, M. S. Gordon, J. H. Jensen, S. Koseki, N. Matsunaga, K. A. Nguyen, S. Su, T. L. Windus, M. Dupuis, J. A. Montgomery, Jr. *J. Comput. Chem.* **14**, 1347 (1993).
23. Gaussian 03, Revision B.03, M. J. Frisch, G. W. Trucks, H. B. Schlegel, G. E. Scuseria, M. A. Robb, J. R. Cheeseman, J. A. Montgomery, Jr., T. Vreven, K. N. Kudin, J. C. Burant, J. M. Millam, S. S. Iyengar, J. Tomasi, V. Barone, B. Mennucci, M. Cossi, G. Scalmani, N. Rega, G. A. Petersson, H. Nakatsuji, M. Hada, M. Ehara, K. Toyota, R. Fukuda, J. Hasegawa, M. Ishida, T. Nakajima, Y. Honda, O. Kitao, H. Nakai, M. Klene, X. Li, J. E. Knox, H. P. Hratchian, J. B. Cross, C. Adamo, J. Jaramillo, R. Gomperts, R. E. Stratmann, O. Yazyev, A. J. Austin, R. Cammi, C. Pomelli, J. W. Ochterski, P. Y. Ayala, K. Morokuma, G. A. Voth, P. Salvador, J. J. Dannenberg, V. G. Zakrzewski, S. Dapprich, A. D. Daniels, M. C. Strain, O. Farkas, D. K. Malick, A. D. Rabuck, K. Raghavachari, J. B. Foresman, J. V. Ortiz, Q. Cui, A. G. Baboul, S. Clifford, J. Cioslowski, B. B. Stefanov, G. Liu, A. Liashenko, P. Piskorz, I. Komaromi, R. L. Martin, D. J. Fox, T. Keith, M. A. Al-Laham, C. Y. Peng, A. Nanayakkara, M. Challacombe, P. M. W. Gill, B. Johnson, W. Chen, M. W. Wong, C. Gonzalez, and J. A. Pople, Gaussian, Inc., Pittsburgh PA, 2003.
24. a) Landolt-Bornstein, in *Structure Data of Free Polyatomic Molecules*, edited by W. Martienssen (Springer-Verlag, Berlin, 1998), Vol. II/25A; b) W. B. Olson, R. H. Hunt, B. W. Young, A. G. Maki, and J. W. Braut, *J. Mol. Spectrosc.* **127**, 12 (1988); c) W. B. Cook, R. H. Hunt, W. N. Shelton, and F. A. Flaherty, *J. Mol. Spectrosc.* **171**, 91 (1995); d) A. Perrin, A. Valentin, J.-M. Flaud, C. Camy-Peyret, L. Schriver, A. Schriver, and Ph. Arcas, *J. Mol. Spectrosc.* **171**, 358 (1995); e) C. Camy-Peyret, J.-M. Flaud, J. W. C. Johns, and M. No<sup>o</sup>el, *J. Mol. Spectrosc.* **155**, 84 (1992); f) T. Shimanouchi, *J. Phys. Chem. Ref. Data* **6**, 993 (1977); g) S. Bashkin and J. O. Stoner, *Atomic Energy Levels and Grotrian Diagrams* (North-Holland, Amsterdam, 1975), Vol. 1; h) K. P. Huber and G. Herzberg, *Molecular Spectra and Molecular Structure* (Van Nostrand Reinhold, New York, 1979), Vol. 4; i) G. Herzberg, *Molecular Spectra and Molecular Structure* (Van Nostrand Reinhold, New York, 1966), Vol. 3; j) W. E. Thompson and M. E. Jacox, *J. Chem. Phys.* **91**, 3826 (1989).
25. Available from <http://www.nist.gov>.
26. M. W. Schmidt and M. S. Gordon, *Annu. Rev. Phys. Chem.* **49**, 233 (1998).
27. R. Atkinson, D. L. Baulch, R. A. Cox, R. F. Hampson, Jr., J. A. Kerr, and J. Troe, *J. Phys. Chem. Ref. Data* **21**, 1125 (1992).
28. T. L. Nguyen, A. M. Mebel, and S. H. Lin, *J. Chem. Phys.* **114**, 10816 (2001).
29. J. Shu, J. J. Lin, C. C. Wang, Y. T. Lee, X. Yang, T. L. Nguyen, and A. M. Mebel, *J. Chem. Phys.* **115**, 7 (2001).